Theory and Simulation of Neoclassical Transport Processes, with Local Trapping

Daniel H. E. Dubin

Department of Physics, University of California at San Diego, La Jolla, CA USA 92093-0319

Abstract.

Neoclassical transport is studied using idealized simulations that follow guiding centers in given fields, neglecting collective effects on the plasma evolution, but including collisions at rate ν. For simplicity the magnetic field is assumed to be uniform; transport is due to asymmetries in applied electrostatic fields. Also, the Fokker-Planck equation describing the particle distribution is solved, and the predicted transport is found to agree with the simulations. Banana, plateau, and fluid regimes are identified and observed in the simulations. When separate trapped particle populations are created by application of an axisymmetric squeeze potential, enhanced transport regimes are observed, scaling as $\sqrt{\nu}$ when $\nu < \omega_0 < \omega_b$ and as $1/\nu$ when $\omega_0 < \nu < \omega_b$ where ω_0 and ω_b are the rotation and axial bounce frequencies, respectively. These regimes are similar to those predicted for neoclassical transport in stellarators.

Irreversible processes driven by the interaction of a plasma with static electric and/or magnetic fields are of central importance in plasma theory and experiment. For example, in the theory of neoclassical transport, a magnetically confined plasma interacts with static electric and/or magnetic field asymmetries, causing irreversible flows of particles, momentum, and energy across the magnetic field [1, 2, 3, 4]. While neoclassical theory is well developed, experiments have never fully tested the theory. In neutral plasma experiments, early work on quiescent discharges was broadly consistent with neoclassical theory [5]; but in many experiments neoclassical transport is masked by anomalous transport caused by nonlinear saturation of collective plasma instabilities. In non-neutral plasma experiments, where such instabilities are absent, detailed measurements of transport over the course of several decades have still failed to make close contact with neoclassical theory [6, 7, 8, 9]. Interpretation of experimental results is often complicated by the interplay of multiple effects, even in the simplest experimental design.

In order to clarify the reasons behind observed discrepancies between neoclassical theory and experiments in nonneutral plasmas, the theory has recently been recast to consider electrostatic field errors of the type typically encountered in nonneutral experiments, and simplified for cylindrical geometry and uniform magnetic field [10]. In this recent work, specific examples were analyzed theoretically and compared to simulations that measure the transport. To further simplify the theory and simulations, plasma shielding effects on the asymmetry potentials were neglected. A local approximation to the kinetic equation, valid in the transport limit where the field error potential is much smaller than the plasma temperature, allowed the determination of local transport coefficients that link dissipative cross- field particle, momentum and energy fluxes to

plasma rotation, parallel velocity, and temperature and velocity gradients. In particular, temperature-gradient-driven particle flux can be important if the gradient is sufficiently large. In non-neutral plasma experiments such large temperature gradients often develop naturally during the transport process itself, as the plasma expands radially and converts some of its electrostatic potential energy into heat.

In each example considered, the transport simulations agreed with the theory. However, such detailed comparisons require rather precise knowledge of the plasma potential, both of the zeroth-order equilibrium and the asymmetry. For instance it was observed that if, in the zeroth order equilibrium, there exists separate trapped particle populations caused by an azimuthally symmetric squeeze potential, and if the rotation frequency is small compared to the bounce frequency, the transport is strongly modified from the banana and plateau regime predictions. New $1/\nu$ and $\sqrt{\nu}$ regimes were found similar to those predicted in neoclassical transport theory for toroidal plasmas [11, 8]. Even a small population of such trapped particles completely changes the magnitude and scaling of the transport from theory predictions in the absence of trapping. Furthermore, theory presently under development suggests that small θ-asymmetries in the squeeze potential can further increase the transport due to chaotic separatrix crossing.

This paper briefly describes the theory and simulations presented in Ref. [10]. The transport theory assumes that a guiding center description of the particle motion is sufficient. In the absence of collisions, the guiding center position is described by cylindrical coordinates (r, θ, z), and only the momentum parallel to the magnetic field p_z is followed; the kinetic energy perpendicular to the field is an adiabatic invariant and is not required. Equations of motion for the guiding center are of Hamiltonian form:

$$\frac{d\theta}{dt} = \frac{\partial H}{\partial p_\theta}, \quad \frac{dp_\theta}{dt} = -\frac{\partial H}{\partial \theta},$$

$$\frac{dz}{dt} = \frac{\partial H}{\partial p_z}, \quad \frac{dp_z}{dt} = -\frac{\partial H}{\partial z} \tag{1}$$

where we follow

$$p_\theta = eBr^2/2c \tag{2}$$

rather than r because p_θ is canonically conjugate to θ, and where the Hamiltonian H is given by

$$H(\theta, p_\theta, z, p_z) = \frac{p_z^2}{2m} + \phi(\theta, p_\theta, z), \tag{3}$$

where ϕ is the electrostatic potential energy. We assume that this potential is time independent and of the form

$$\phi(p_z, \theta, z) = \phi_0(p_\theta, z) + \delta\phi(p_\theta, \theta, z) \tag{4}$$

where ϕ_0 is the equilibrium potential of the plasma, including cylindrically-symmetric external confinement fields, and $\delta\phi$ is an applied asymmetry potential that is responsible for the transport. The theory assumes that $\delta\phi \ll T$, where T is the plasma temperature, in order that the plasma expansion is a slow transport process.

The single particle orbits described by Eq. (1) are by themselves insufficient to describe neoclassical transport processes; the potentials in typical experiments are such

that these orbits remain confined. Collisions are needed to describe plasma loss, and are added to the theory by way of the Fokker-Planck equation for the particle distribution function $f(\theta, p_\theta, z, p_z, t)$:

$$\frac{\partial f}{\partial t} + \dot{\theta}\frac{\partial f}{\partial \theta} + \dot{p}_\theta \frac{\partial f}{\partial p_\theta} + \dot{z}\frac{\partial f}{\partial z} + \dot{p}_z \frac{\partial f}{\partial p_z} = \hat{C}f \tag{5}$$

where here we assume a collision operator of the form

$$\hat{C}f = D\frac{\partial}{\partial p_z}\left(\frac{\partial f}{\partial p_z} + \frac{p_z - mV_b}{mT_b}f\right) \tag{6}$$

and where D is the diffusion coefficient for parallel momentum, V_b is the parallel velocity of a background species with which the plasma is colliding (usually taken to be zero), and T_b is the temperature of the background. Other forms of the collision operator could be used (see Ref. [10] for some examples), but Eq. (6) is particularly easy to simulate.

Equation (5) can be solved in the limit $\delta\phi \ll T$ to obtain expressions for the fluxes of particles, energy, and momentum across the magnetic field due to the asymmetry. The fluxes are linearly related to V_b, to gradients (if any) in V_b and T_b, and to the fluid plasma rotation frequency ω_r, defined as

$$\omega_r = -\frac{\partial\bar{\phi}}{\partial p_\theta} - \frac{T_b}{\bar{n}}\frac{\partial\bar{n}}{\partial p_\theta}, \tag{7}$$

where $\bar{\phi}$ is the θ and z-averaged potential (weighted by the plasma density) and $\bar{n}$ is the θ and z-averaged density. The first term is the average $\mathbf{E} \times \mathbf{B}$ drift and the second term is related to the plasma diamagnetic drift; here we note that when $\delta\phi \ll T$, T_b is nearly the same as T because plasma heating due to the asymmetry is weak, so we could replace T_b by T in Eq. (7) [this was done in Ref. [10] in the sections of the paper that employed the collision operator given by Eq. (6)]. In particular, radial particle flux Γ_r is linearly related to rotation via a transport coefficient μ_{11}:

$$\Gamma_r = \frac{c}{eBr}\mu_{11}\omega_r = -\left(\frac{c}{eBr}\right)^2 \mu_{11}\left(\frac{\partial\bar{\phi}}{\partial r} + \frac{T_b}{\bar{n}}\frac{\partial\bar{n}}{\partial r}\right) \tag{8}$$

where we have used Eqs. (3) and (7) to connect the flux to the mobility (the first term) and diffusive (the second term) fluxes. Many (15) other transport coefficients occur in the theory but will not be discussed here.

Solutions for μ_{11} were compared to particle simulations in various cases. The simulations directly measured the diffusion and mobility fluxes to provide independent measures of μ_{11}. In these simulations the Hamiltonian equations of motion given by Eq. (1) are numerically integrated forward in time, but the parallel force law is modified in order to include a nonconservative collisional drag term,

$$dp_z/dt = -\partial H/\partial z - \nu\, p_z \tag{9}$$

where ν is the collision frequency, related to the momentum diffusion coefficient D in Eq. (6) by $D = mT_b\nu$. The equations of motion are integrated numerically using a

4th order Runge-Kutta method with constant time stepsize Δt. After every time step, a random momentum is added to p_z taken from the range $[-p_0, p_0]$ in order to simulate the effect of random forcing due to the collisions. The theory of Brownian motion then implies a relation between the background temperature and the simulation parameters, assuming that $\nu \Delta t \ll 1$:

$$T_b = \frac{p_0^2}{6m\nu\Delta t}. \tag{10}$$

The simulations follow $N \gg 1$ particles starting at the same radius with random z, p_z and θ taken from a Boltzmann distribution $\exp(-H/T_b)$. The following two quantities are evaluated in order to measure mobility and diffusion:

$$\langle \delta r \rangle = \sum_{i=1}^{N} [r_i(t) - r_i(0)] \tag{11}$$

and

$$\langle \delta r^2 \rangle = \sum_{i=1}^{N} [r_i(t) - r_i(0)]^2. \tag{12}$$

The radial mobility coefficient $\mu_r = (c/eBr)^2 \mu_{11}$ is related to the rate of change of the mean radial position change through

$$\bar{n}\frac{d}{dt}\langle \delta r \rangle = \mu_r \bar{E}_r \tag{13}$$

and the radial diffusion coefficient $D_r = (c/eBr)^2 (T_b/\bar{n})\mu_{11}$ is related to the mean square change of radial position:

$$\frac{d}{dt}\left[\langle \delta r^2 \rangle - \langle \delta r \rangle^2\right] = 2D_r. \tag{14}$$

An example of such an evaluation of μ_{11} is shown in Fig. 1. The Hamiltonian used here is

$$H = -\omega_0 p_\theta + \frac{p_z^2}{2m} + \varepsilon\cos(\ell\theta + kz) \tag{15}$$

where ω_0 is the $\mathbf{E} \times \mathbf{B}$ rotation frequency and the field asymmetry is taken to be a single wave with amplitude ε. In this example, $\omega_0 = k\bar{v}$ so the mobility flux is relatively easy to measure; in other cases with smaller values of ω_0 it is easier to measure diffusion in the simulations. Measuring the mobility and diffusive fluxes for different values of the collision frequency allow one to map out the standard banana, plateau and fluid regimes, as shown in Fig. 2 . Also shown in the figure are the theory predictions for the transport in these regimes. One can see that the simulations follow the theory closely.

The scaling of the transport with experimental parameters in each regime can be understood from fairly simple arguments. For large collision frequencies, $\nu > k\bar{v}$, where $\bar{v} \equiv \sqrt{T/m}$, an analysis based on fluid equations provides the transport coefficients [10]. In this fluid regime, radial particle transport is primarily caused by dissipation associated with compression and expansion of the plasma as it rotates through the field error. Temperature and velocity gradients can also lead to irreversible fluxes of particles, energy and momentum as the field error transports particles across the magnetic field.
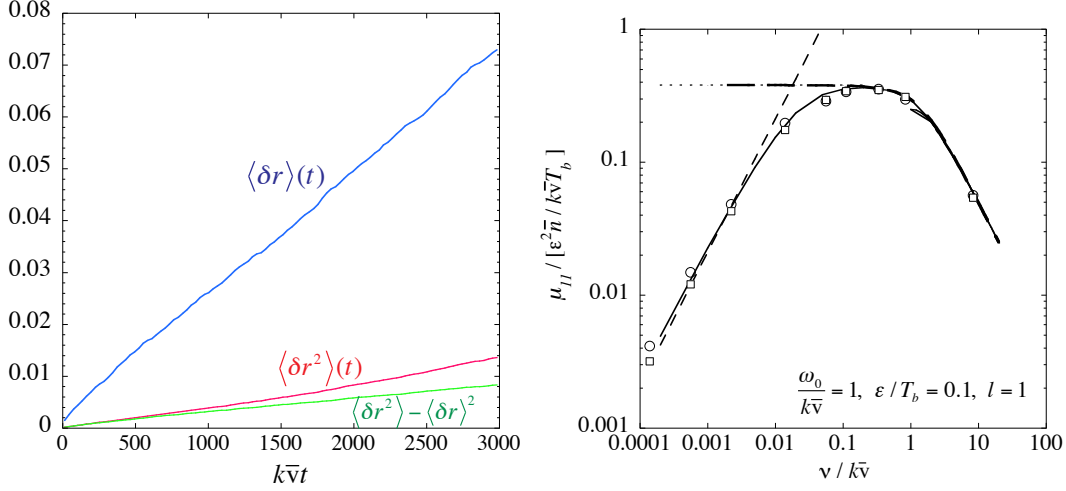
FIGURE 1. Mean and mean square change in radius for a simulation of $N = 3000$ particles following Hamiltonian (15) with $\omega_0/k\bar{v} = 1$, $\varepsilon/T_b = 0.1$, $\ell = 1$, and $\nu/k\bar{v} = 0.002$. Distances are in units of k.

FIGURE 2. Transport coefficient μ_{11} versus collision frequency for Hamiltonian (15), obtained by mobility measurements (squares) and diffusion measurements (dots). Lines are theory in different limits. Solid line is a full nonlinear solution of Eq. (5) for μ_{11}; thick dashed line linearizes the solution for f in $\delta\phi$; thin dashed line is the banana limit; dotted line is the plateau limit; and dot-dashed line (barely visible) is the fluid limit.

For small collision frequencies, $\nu < (\varepsilon/T)^{3/2}k\bar{v}$, transport coefficients are linear functions of ν [12, 13]. The scaling of the radial diffusion coefficient D_r in this "banana regime" may be understood from the following argument. Particles become trapped in the field asymmetry when they have an axial velocity v_z that satisfies

$$\frac{m}{2}(v_z - \ell\omega_0/k)^2 < \varepsilon. \tag{16}$$

The trapped particles execute axial oscillations in the field error at roughly the trapping frequency $\omega_T = \sqrt{k^2\varepsilon/m}$. In these axial trapping oscillations, the particles also drift radially, with a radial "banana orbit" width $\Delta r \sim \ell\sqrt{2\varepsilon/m}/kr\Omega_c$ where $\Omega_c = eB/mc$. This estimate follows from the product of the radial drift velocity $\ell c\varepsilon/eBr$ and the period ω_T^{-1} of the oscillation. Transport occurs as particles become collisionally detrapped and then retrapped.

The size of the step in this process is Δr. The time between steps is the time Δt required to be detrapped from the banana orbit, $\Delta t \sim \varepsilon/(\nu T)$ (the time needed to diffuse in energy by order ε). The radial particle diffusion coefficient D_r is therefore roughly

$$D_r \sim f\frac{\Delta r^2}{\Delta t} \tag{17}$$

where f is the fraction of particles that take part in the banana orbits, of order $f \sim e^{-\ell^2\omega_0^2/2k^2\bar{v}^2}\sqrt{\varepsilon/T}$ for a Maxwellian distribution. Putting these estimates together yields

$$D_r \sim \nu\sqrt{\frac{\varepsilon}{T}}\frac{\ell^2\bar{v}^2}{k^2r^2\Omega_c^2}e^{-\ell^2\omega_0^2/2k^2\bar{v}^2} \tag{18}$$

in the banana regime. A more rigorous derivation [10] yields Eq. (18) with a numerical coefficient of 1.1. This is plotted in Fig. 2 as a thin dashed line. This banana regime estimate is sensible only when the particles are able to execute a full trapping oscillation before they are collisionally detrapped: this requires $\omega_T \Delta t \gtrsim 1$, which implies

$$(\varepsilon/T)^{3/2} k\bar{v} > v \tag{19}$$

for the banana regime.

For $k\bar{v}(\varepsilon/T)^{3/2} < v < k\bar{v}$, the transport is in the plateau regime. Trapped particles no longer complete an entire banana orbit, so the size of the radial step is reduced to $\Delta r \omega_T \Delta t$. The diffusion coefficient is now given by

$$D_r \sim f_v \frac{(\Delta r \omega_T \Delta t)^2}{\Delta t} \tag{20}$$

where f_v is the fraction of particles in resonance with the error,

$$f_v \sim e^{-\ell^2 \omega_0^2 / 2k^2 \bar{v}^2} / (k\bar{v}\Delta t). \tag{21}$$

This estimate yields the plateau regime diffusion coefficient

$$D_r \sim \left(\frac{\varepsilon}{T}\right)^2 \frac{\ell^2 \bar{v}^3}{kr^2 \Omega_c^2} e^{-\ell^2 \omega_0^2 / 2k^2 \bar{v}^2}. \tag{22}$$

A rigorous derivation of plateau regime transport for Hamiltonian (15) yields Eq. (22) with coefficient $\sqrt{\pi/8}$. This is plotted in Fig. 2 as a dotted line, and in Fig. 4 as a dashed line.

In this example, the particle motion is unconstrained in the z direction. More typical of many nonneutral plasma experiments are finite length plasmas confined in z by applied potentials. In the next example the transport in such a plasma is simulated using the following Hamiltonian:

$$H = \frac{p_z^2}{2m} - \omega_0 p_\theta + T_b \left(\frac{z}{L}\right)^8 + \varepsilon \cos\theta \sin kz \tag{23}$$

where L is the plasma length, taken to be $kL = 4.217$.

The particle transport is measured in the same way as before, and shows similar behavior compared to the previous example, with banana, plateau, and fluid regimes apparent, and theory and simulations are again in agreement (see Fig. 3). It is important to note however that the transport in the banana and plateau regimes is a fairly sensitive function of the plasma parameters. For instance, a plot of the plateau regime value for μ_{11} is displayed in Fig. 4, evaluated for both the infinite length example of Eq. (15) and the finite length example of Eq. (23). Although the field asymmetries are very similar in the two examples, the transport displays considerably more structure in the second case due to the complex interplay between different bounce harmonics. In interpreting experiments, this shows that the plasma parameters such as rotation frequency and axial potential must be very well characterized in order for theory to be able to make useful predictions of the transport.
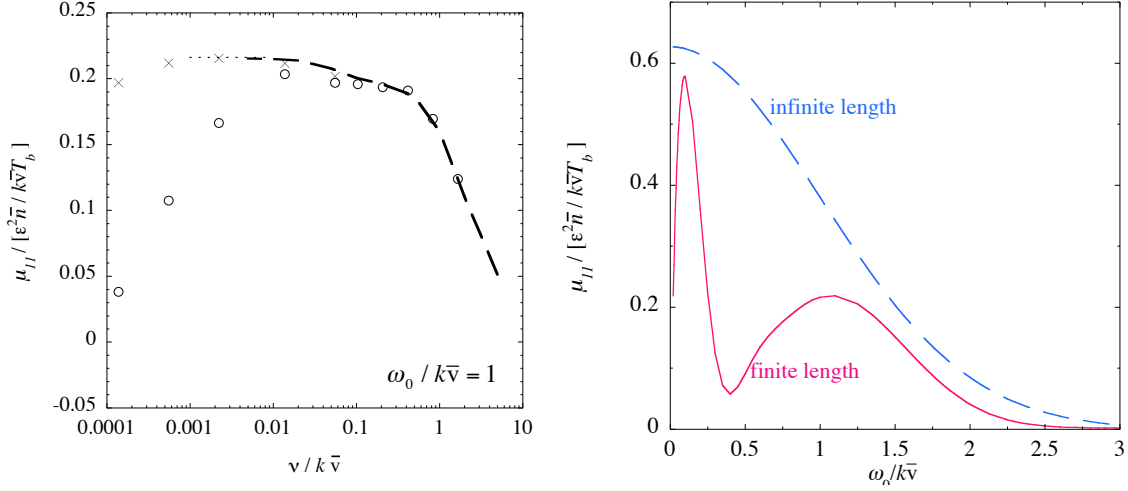
FIGURE 3. Transport coefficient μ_{11} versus collision frequency for finite length Hamiltonian (23), using simulations of diffusion for $\varepsilon/T_b = 0.02$ (dots) and $\varepsilon/T_b = 0.002$ (crosses). Thick dashed line is the theory solution of Eq. (5) for μ_{11} when f is linearized in $\delta\phi$; the dotted line is the plateau regime limit.

FIGURE 4. Plateau regime limits versus rotation frequency for the infinite length case of Hamiltonian (15) (dashed) and the finite length case of Hamiltonian (23) (solid).

Sensitive dependence of the transport on the applied potentials is also exemplified in the next case considered, in which the addition of an axisymmetric squeeze potential that creates trapped particle populations that are separated by a separatrix is found to completely change the magnitude and scaling of the transport, even when the fraction of trapped particles is small. The Hamiltonian in this case is taken to be

$$H = \frac{p_z^2}{2m} - \omega_0 p_\theta + T_b \left(\frac{z}{L}\right)^8 + V_{sq} e^{-50(kz)^4} + \varepsilon \cos\theta \sin kz \tag{24}$$

where V_{sq} is the magnitude of the applied squeeze potential. When the plasma rotation frequency ω_0 is small compared to $k\bar{v}$, two new transport regimes occur, scaling with collision frequency as $1/\nu$ and $\sqrt{\nu}$.

The $1/\nu$ regime occurs when $\omega_0 < \nu < k\bar{v}$, and the transport can be understood from the following scaling argument: Since the field error potential happens to be an odd function of z, low-energy particles trapped in the $z < 0$ well created by the squeeze potential experience the opposite field error potential from those trapped in the $z > 0$ well. As a result, the $\mathbf{E} \times \mathbf{B}$ drift orbits of particles in these two wells are displaced relative to one another, and relative to untrapped particles. The magnitude Δr of the radial displacement is of order

$$\Delta r \sim \frac{\varepsilon}{m\Omega_c \omega_0 r}. \tag{25}$$

As particles wander in energy due to collisions they become detrapped and then retrapped on a timescale of order ν^{-1}, assuming that V_s is of order T_b. Since particles only complete a fraction of a drift orbit in this time, the magnitude of the radial drift step
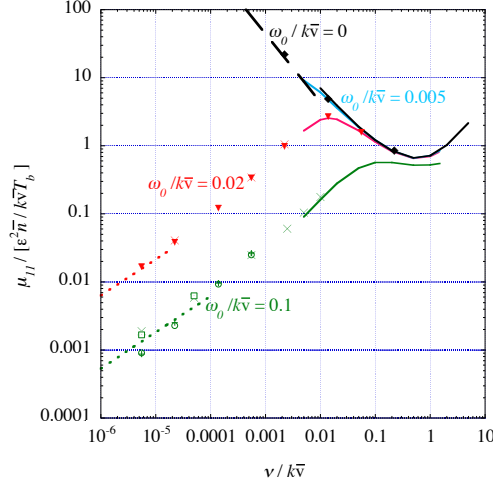
FIGURE 5. Transport coefficient μ_{11} versus collision frequency for a plasma with added squeeze given by Hamiltonian (24), with $V_{sq}/T = 0.5$, at four rotation frequencies. Symbols display simulation results. The dashed line is the $1/\nu$ regime result of Eq. (27); the dotted lines are the $\sqrt{\nu}$ regime results. Solid lines are solutions of Eq. (5) for μ_{11}, linearizing f in $\delta\phi$.

that they make is of order $\Delta r\,\omega_0/\nu$. The radial diffusion coefficient is then

$$D_r \sim \nu \left(\frac{\Delta r\omega_0}{\nu} \right)^2 \sim \frac{1}{\nu} \left(\frac{\varepsilon}{m\Omega_c r} \right)^2. \qquad (26)$$

In the $1/\nu$ regime, the particle diffusion increases as ν decreases,[14, 15] up to the point where $\nu < \omega_0$.

A more rigorous derivation of the transport in the $1/\nu$ regime yields, for Hamiltonian (24) with squeeze potential $V_{sq} = 0.5T_b$,

$$\mu_{11} = 0.0444 \frac{\bar{n}\varepsilon^2}{\nu T_b}. \qquad (27)$$

This result is displayed in Fig. 5 and matches the simulations when ω_0 is sufficiently small.

However, when ν falls below ω_0, transport begins to decrease with decreasing ν, as the transport enters the $\sqrt{\nu}$ regime. The transport in this regime can be understood in the following way. Particles trapped by the squeeze potential feel a different bounce-averaged field error than particles that are untrapped. The untrapped particles, bouncing rapidly from one end of the plasma to the other, average out the asymmetry potential so that, on average, they feel no net effect from the asymmetry. However, trapped particles on either side of the squeeze feel opposite asymmetry potentials, $\delta\bar{\phi} \sim \pm\varepsilon\cos\theta$. This difference between trapped and untrapped particles creates, in the absence of collisions, a discontinuity in the distribution function f at the separatrix. In the frame of the plasma, the discontinuity oscillates in time as the plasma rotates through the asymmetry. If collisions are now taken into account, the oscillating discontinuity is smoothed out by diffusion of particles in energy, over a boundary layer around the separatix of width

$\sqrt{T V_{sq} \nu / \omega_0}$. This sort of boundary layer is common in driven diffusion problems, where an oscillating source at frequency ω_0 creates an oscillating particle distribution that spreads from the source a distance of order $\sqrt{D/\omega_0}$, where D is the diffusion coefficient.

This oscillating distribution creates radial particle transport in the following way. Every rotation period, particles in the boundary layer diffuse back and forth across the separatrix, going from trapped to untrapped orbits. When the particles are trapped, they take a radial step of approximate magnitude given by Eq. (25). However, the sign of this step is random because particles are equally likely to be trapped on either side of the squeeze potential. The diffusion coefficient is the rate at which these random steps are taken, given in this case by the rotation frequency, multiplied by the square of the step, and finally multiplied by the fraction of particle participating, ie. the fraction of particles in the boundary layer:

$$D_r \sim \omega_0 \Delta r^2 \times \sqrt{\nu / \omega_0}\, e^{-V_{sq}/T} \sim \sqrt{\nu \omega_0}\, e^{-V_{sq}/T} \left(\frac{\varepsilon}{m \Omega_c \omega_0 r} \right)^2 . \qquad (28)$$

The scaling of this estimate for the radial diffusion coefficient agrees with a rigorous transport calculation shown in Fig. 5 as the dashed lines for two different values of the rotation frequency. Note that this transport remains finite even when $V_{sq} \ll T$, provided that the energy width of the boundary layer is small compared to V_{sq}, i.e. $\nu / \omega_0 < V_{sq}/T$. Thus, even small squeeze potentials can have a significant impact on the transport.

Finally, we note that the transport can be further enhanced if the squeeze potential is itself asymmetric in θ. In this case as particles near the separatix energy rotate in θ, they can become trapped and untrapped along *collisionless* orbits. This collisionless transport mechanism will be explored further in future work.

ACKNOWLEDGMENTS

REFERENCES

1. F.L. Hinton and R.D. Hazeltine, Rev. Mod. Phys. **48**, 239 (1976).
2. H.E. Mynick, Phys. Plasmas **13**, 058102 (2006).
3. F.L. Hinton and M.N. Rosenbluth, Phys. Fluids **16**, 836 (1983).
4. R.D. Hazeltine, F.L. Hinton, and M.N. Rosenbluth, Phys. Fluids **16**, 1645 (1973).
5. T. Ohkawa, J.R. Gilleland and T. Tamano, Phys. Rev. Lett. **28**, 1107 (1972).
6. J.H. Malmberg and C.F. Driscoll, Phys. Rev. Lett. **44**, 654 (1980).
7. C.F. Driscoll and J.H. Malmberg, Phys. Rev. Lett. **50**, 167 (1983).
8. D.L. Eggleston and B. Carillo, Phys. Plasmas **10**, 1308 (2003).
9. A.A. Kabantsev, J.H. Yu, R.B. Lynch and C.F. Driscoll, Phys. Plasmas **10**, 1628 (2003).
10. D.H.E. Dubin, Phys. Plasmas **15**, 072112 (2008).
11. M.N. Rosenbluth, D.W. Ross, and D.P. Kostomarov, Nucl. Fusion **12**, 3 (1972).
12. A.A. Galeev and R.Z. Sagdeev, Sov. Phys. JETP **26**, 233 (1968).
13. M.N. Rosenbluth, R.D. Hazeltine and F.L. Hinton, Phys. Fluids **15**, 116 (1972).
14. H.E. Mynick, Phys. Plasmas **13**, 058102 (2006).
15. A. Gibson *et al.*, Plasma Phys. **11**, 121 (1969).